Investigation of Parameters Affecting the Geometry of Red Blood Cell Using Low-Dimension Model in Dissipative Particle Dynamics

Somaye Yaghoubi[1,2]

[1]Department of Mechanical Engineering- Najafabad Branch, Islamic Azad University, Najafabad, Iran
[2]Aerospace and Energy Conversion Research Center- Najafabad Branch, Islamic Azad University, Najafabad, Iran
(s.yaghoubi@pmc.iaun.ac.ir)

Abstract

Approximately one half of the blood flow is made up of the Red Blood Cells (RBCs). Moreover, the geometry of the RBCs relative to the vessel diameter greatly effect on the physics and dynamics of the blood flow. It means the quantitative understanding through the vessels is important in multifarious pathologies. To simulate RBCs, one of the modelling concerns is related to the details required for the sufficient accuracy and another is about the cost of computational methods. The mesoscopic models of RBCs combined both parameters accuracy and optimality. Then to achieve some of these goals in this study a numerical model called Low-Dimensional (LD) model along with DPD method are used to simulate Red Blood Cells, RBCs, in blood flows. LD-DPD model is developed due to new formulation of single particle in DPD and is able to capture the essential mechanics properties of these suspensions economically because of the low number of particles. The advantage of LD model is the use of spherical particles compared to the standard DPD which assumes point particles. For instance, in this study, to simulate a RBC, only10 colloidal particles are required. Also it is proved in this work different parameters are effective to determine the RBC radius and using this method, it is easy to investigate them until to match this simulation with the real one.

Keywords: blood flow, dissipative particle dynamics, low-dimensional model, red blood cells, spherical particles
Article history: Received 01-Feb-2022; Revised 09-Feb-2022; Accepted 27-Feb-2022.

https://doi.org/10.30495/ijsee.2022.1951431.1170

1. Introduction

The amount of the blood flow which is occupied by the red blood cells (RBCs), is considerable (approximately one half of the blood flow) [1,2]. A normal red blood cell has deformable biconcave shape [3,4]. The size and deformability of the RBCs relative to the vessel diameter and then their geometry greatly effect on the physics and dynamics of the blood flow. Then in multifarious pathologies, the blood flow has a key role because of the RBCs. For instance, the blood flow can be modeled as a homogeneous fluid in vessels with diameters more than 200 μm [5,6]. However, for modeling smaller vessels, such as arterioles and venues, it is necessary to consider the blood flow as a two-phase suspension of RBCs [7,8]. Therefore, for simulating the blood flow, quantitative understanding through the vessels is important [9,10]. To simulate blood flow a number of numerical models have been developed based on the molecular level [11,12], description at a continuum level [13,14] and also at the mesoscopic scale [15,16].

Combination of nonlinear solid deformations and fluid flow in continuum models often was annoyed because of significant computational cost. Detailed molecular models are also confined by the required computational expense. With these circumstances, mesoscopic models of RBCs combine both parameters accuracy and optimality. Therefore, modelling of red blood cells is done using mesoscopic models [17,18].

In several works the red blood cells was exhibited by a network of springs considering the

bending force and conservation of surface-area and volume for the body [19,20].

To predict the dynamics of a solid particle in a post stenotic blood vessel region a numerical model is developed in [21]. In this research, discrete phase model (DPM) based on a Lagrangian approach is used and spherical particles are injected in the flow from the stenosis and tracked

A multiscale numerical model which is able to predict mechanical, rheological and dynamical properties for Red blood cells is presented in [22]. These properties are in agreement with experiments. A comparison with the rheological properties of the membrane and results obtained for example in optical magnetic twisting cytometry is done. These results are obtained for example in optical magnetic twisting cytometry. It is find for the accurate representation of the rheological and dynamical properties of the RBC, a purely elastic membrane model is not sufficient and an accurate viscoelastic model for the membrane is necessary.

To examine some parameters such as the cell layer development process, the effects of cell deformability and aggregation on hemodynamic and hem-rheological behaviours, in [23] immersed-boundary lattice Boltzmann algorithm is used. In this work Morse potential is used to model the aggregation among cells. Also in providing valuable information on microscopic blood flows immersed-boundary lattice Boltzmann numerical model was useful.

To investigate RBC motion numerically in [24] a combination of mesoscale methods is used. The low dimensional-RBC based on dissipative particle dynamics method combined with a hybrid lattice Boltzmann method-immersed boundary method. In this combined model the computational cost decrease compared to the microscale models. Also the combined method was able to model the deformation of red blood cell accurately. Then as a benchmark test, the deformation index as the function of the capillary number of RBC motion through a narrow cylindrical tube has been performed. Therefore, the relationship between the RBC diameter and the force value derived by the low dimensional-RBC method is compared with numerical and experimental data.

Despite the promising results of above mentioned methods, their high computational cost for modelling the vessels with diameters larger than 20-50 μm is still inconvenient. Therefore, the simulation methods that provide a mesoscale model of blood flow in large vessels are very limited in numbers. In the biological processes associated with small arteries, which usually require an explicit modelling of red blood cells, it is common to use molecular-level models with each single red blood cell expressed with hundreds to tens of thousands of particles. Running such multi-particle simulation will be very expensive; for example, simulating the flow in a 500μm long and 50μm in diameter arteriole in which only 35% of volume has been occupied by RBCs require simulating millions to hundreds of millions of particles [25,26].

In the present work, we use a low-dimension (LD) model based on dissipative particle dynamics (DPD) as an effective approach to overcome the problem of high computational cost associated with the simulation of red blood cells. This RBC modelling procedure consists of only 10 colloidal particles that have been attached to each other by worm-like chain (WLC) springs. Simulation of each colloidal particle starts with a single particle of DPD based on new DPD formulation, and is then augmented by adding non-central dissipative shear forces between the particles in the standard DPD, where the angular momentum among particles is also conserved by these forces [27,28].

To model the bending rigidity of red blood cells, bending resistance is incorporated into the ring model as an angular bending force depending on the angle between two consecutive spring. In fact, a big advantage of this model over existing mesoscale methods is the presence of spherical particles with non-zero volume (unlike the methods such as DPD which assume the particles as volume-less points). In this model, the number of particles required for simulation and thus the computational cost associated with modelling of larger vessels are decreased based on assumption of a radius for each particle. Therefore, particle radius can be counted as one of the most fundamental parameters of this model. It needs to be mentioned that in this model, the particle radius is considered as an input parameter and plays a decisive role, for example, in calculating the values of the forces and momenta applied to each particle. In addition, during scaling and converting the DPD dimensions into physical units, the radius of red blood cell needs to be known. Contributions of this research to the literature include determination of desirable particle radius, factors and parameters affecting this radius, and the mechanism of these effects. The results obtained for the RBC radius are evaluated and validated according to the findings regarding equilibrium length (spring length) between two adjacent colloids in a blood cell as well as geometrical investigation, and will be described in detail.

This introduction discussed the importance of simulation of blood cells and vessels, and mentioned the strengths and shortcomings of notable studies previously carried out on this subject. In the second section, the governing equations of the low-dimensional DPD model are introduced, and the model is then used to simulate the red blood cells. In the third section, the radius of red blood cells is

determined, and parameters associated with this radius are investigated. In that section, the equilibrium length between two adjacent colloids in a blood cell is also calculated with respect to these parameters. Then, the accuracy of the results is analysed by geometric arguments. In the last section, the overall conclusions of this work are described.

2. The Low-Dimension Model Based on Dissipative Particle Dynamics

In the present study, the red blood cell is modeled as a ring of 10 colloidal particles connected to each other via worm-like chain (WLC) springs. Each colloidal particle was simulated by a single particle of DPD. In this formulation, the dissipative forces acting on a particle are divided explicitly into two separate components: central and shear (non-central) components. It has been shown that the new formulation of DPD method leads to accurate prediction of hydrodynamic forces and momenta for a single DPD particle and accurate prediction of hydrodynamics of colloidal particles. In the following, we will review this new formulation [29].

The simulation includes a set of particles with mass of m, position of $\vec{r}_i$, linear velocity of $\vec{v}_i$, and angular velocity of $\vec{\Omega}_i$; defined as $\vec{r}_{ij}=\vec{r}_i-\vec{r}_j$, $r_{ij}=|\vec{r}_{ij}|$, $\vec{e}_{ij}=\vec{r}_{ij}/r_{ij}$ and $\vec{v}_{ij}=\vec{v}_i-\vec{v}_j$. The following relations give the force and momentum acting on particle i:

$$\begin{cases}\vec{F}_i=\sum_j \vec{F}_{ij}\\ \vec{T}_i=-\sum_j \lambda_{ij}\vec{r}_{ij}\times\vec{F}_{ij}\end{cases} \quad (1)$$

Here, the factor λ_{ij} (introduced in [30]) is a weight that reflects different contributions of various types of particles (e.g., solvent or colloid) with differing sizes, while the angular momentum is conserved. This factor is defined as follows:

$$\lambda_{ij}=\frac{R_i}{R_i+R_j} \quad (2)$$

If $R_i=R_j$ (where R_i and R_j refer to the radius of the particles i and j, respectively) then $\lambda_{ij}=1/2$. The force applied on particle i by particle j is given by the following equation:

$$\vec{F}_{ij}=F_{ij}^{U}+\vec{F}_{ij}^{T}+\vec{F}_{ij}^{R}+\tilde{F}_{ij} \quad (3)$$

where, $\vec{F}_{ij}^{U}$ is the conservative force, $\vec{F}_{ij}^{T}$ is the translational force, $\vec{F}_{ij}^{R}$ is the rotational force and $\tilde{F}_{ij}$ is the random force, which all will be short range explained. The conservative radial force can have the standard DPD form.

$$\vec{F}_{ij}^{U}=\begin{cases}a_{ij}(1-r_{ij}/r_c)\vec{e}_{ij} & r_{ij}<r_c\\ 0 & r_{ij}\geq r_c\end{cases} \quad (4)$$

where, r_c is the cut-off radius. The translational force is expressed as:

$$\begin{aligned}\vec{F}_{ij}^{T}&=-\left\{g_{ij}^{\wedge}f^{2}(r_{ij})\mathbf{1}+(g_{ij}^{\parallel}-g_{ij}^{\wedge})f^{2}(r_{ij})\vec{e}_{ij}\vec{e}_{ij}\right\}\times\vec{v}_{ij}\\ &=-g_{ij}^{\parallel}f^{2}(r_{ij})(\vec{v}_{ij}\times\vec{e}_{ij})\vec{e}_{ij}\\ &\quad-g_{ij}^{\wedge}f^{2}(r_{ij})[\vec{v}_{ij}-(\vec{v}_{ij}\times\vec{e}_{ij})\vec{e}_{ij}].\end{aligned} \quad (5)$$

This force, namely the drag, is due to the translational velocity $\vec{v}_{ij}$ of particle i relative to j. The mentioned force is decomposed into two components: one along the line connecting the centers of the particles and another perpendicular to that line. The drag coefficients are expressed by $g_{ij}^{\parallel}$ and $g_{ij}^{\wedge}$, respectively, for central and shear components. It should be noted that the central component of the force is the same as dissipative force in the standard DPD. The rotational force is defined by the following equation:

$$\vec{F}_{ij}^{R}=-g_{ij}^{\wedge}f^{2}(r_{ij})\vec{r}_{ij}\times(l_{ij}\vec{W}_i+l_{ji}\vec{W}_j) \quad (6)$$

In addition, the random force is given by the following equation:

$$\tilde{F}_{ij}dt=f(r_{ij})\left\{\frac{1}{\sqrt{3}}s_{ij}^{\parallel}\mathrm{tr}[d\mathbf{W}_{ij}]\mathbf{1}+\sqrt{2}s_{ij}^{\wedge}d\mathbf{W}_{ij}^{A}\right\}\times\vec{e}_{ij} \quad (7)$$

where, $s_{ij}^{\parallel}=\sqrt{2k_BT\,g_{ij}^{\parallel}}$ and $s_{ij}^{\wedge}=\sqrt{2k_BT\,g_{ij}^{\wedge}}$ meaning that the fluctuation-depreciation theorem is satisfied.

The generalized weight function, $f(r)=(1-r/r_c)^s$ with s= 0.25 [31] or $f(r)=1-(r/r_c)^k$ with k=60 [32] are used in (5) to (7). In (7), $d\mathbf{W}_{ij}$ is the matrix of independent Wiener increments, which is assumed to be a symmetric matrix under the influence of particle interactions. When $\gamma_{ij}^{\perp}\equiv 0$, the relations of the standard DPD will be given, in which case the shear component of the forces will be ignored.

Colloidal particles are simulated as single DPD particles and similar to the solvent particles but with a larger size. The particle size can be adjusted by conservative force coefficient a_{ij} [(in (4)]. However, the standard DPD linear force, which is defined by the (4), is too soft for modelling of hard-sphere particles. To solve this problem, in this method, an exponential conservative force is defined for colloid-colloid and colloid-solvent interactions, but solvent-solvent interactions are still modelled with DPD linear force. The use of such hybrid

conservative interactions leads to absence of any overlap between colloidal particles dispersed in the solvent. Moreover, here the time step does not need to be very small, like the time steps required for the Lennard-Jones potential [33]. The conservative force, which is defined as an exponential radial function, is in the form of following formula:

$$F_{ij}^{U} = \begin{cases} \frac{a_{ij}}{1- e^{b_{ij}}}(e^{b_{ij} r_{ij}/r_c^e} - e^{b_{ij}}) & r_{ij} < r_c^e \\ 0 & r_{ij} \geq r_c^e \end{cases} \quad (8)$$

where, a_{ij} and b_{ij} are adjustable parameters and r_c^e is the cut-off radius of the exponential function. This exponential function for the conservative force and also the standard linear force in DPD is plotted in Fig. 1. The size of colloidal particle can be controlled by adjusting the value of a_{ij} in (8).

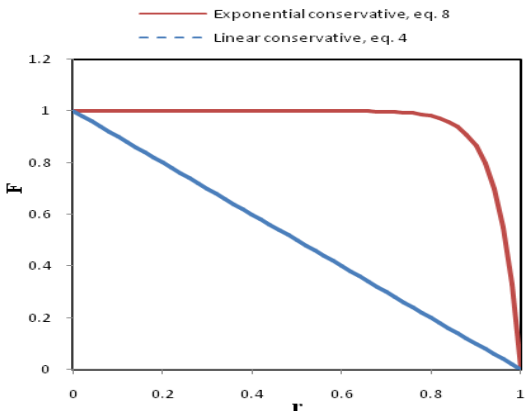

Fig. 1. Distribution of exponential function for conservative force in comparison with the standard linear force (here $r = r_{ij}/r_c^e$ and $F = F_{ij}^{U}/a_{ij}$)

When constructing the model of cell, particles of an RBC are allowed to overlap with each other. This means that colloidal particles of an RBC will continue to interact with each other based on soft standard DPD linear force [(see (4)]. The colloidal particle diameter is chosen to be equal to the radius of the ring; and so the final format for each RBC is in the form of closed-torus shown in Fig. 2. This form has a good agreement with the RBC model provided by Pan [34] and can assure us of the correctness and accuracy of the written code. The worm-like chain (WLC) spring force, which connects all particles in each cell belonging to a red blood cell, is expressed by the following equation [35]:

$$\vec{F}_{WLC}^{U} = \frac{k_B T}{l_p}\left[\frac{1}{4(1-\frac{r_{ij}}{L_{\max}})^2} - \frac{1}{4} + \frac{r_{ij}}{L_{\max}}\right] \quad (9)$$

where, r_{ij} is the distance between two adjacent beads, λ_p is the persistence length, and L_{max} is the maximum allowed length for each spring. Each cell also has a bending resistance, so this bending resistance is inevitably applied in the form of angular bending forces depending on the angle between two adjacent springs in the ring RBC model. This bending force has been derived by differentiation of cosine bending potential in the following form:

$$U_{ijk}^{COS} = k_b[1- \cos q_{ijk}] \quad (10)$$

where, k_b is the bending stiffness, q_{ijk} is the angle between two consecutive springs or the inner product of $\vec{r}_{ij}$ and $\vec{r}_{jk}$. Thus, the bending force acting on particle jis obtained from the differentiation of above mentioned potential:

$$F_j^{COS} = -\frac{\partial U_{ijk}^{COS}}{\partial r_j} \quad (11)$$

The random force coefficients for different interactions can be obtained based on the relationship $s_{ij} = \sqrt{2k_B T\, g_{ij}}$ with $k_B T$ =0.1. The Number density of particles in the solvent and at the walls are considered to be $n_s = n_w$ =3.

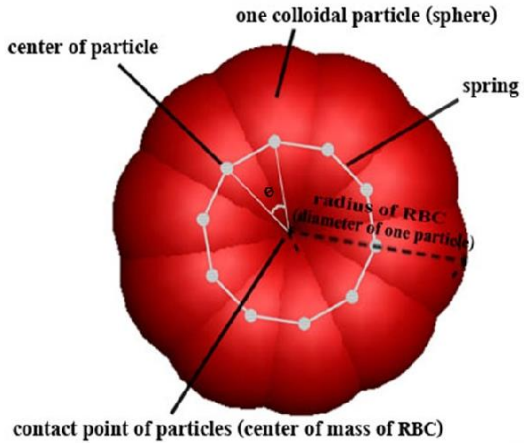

Fig. 2. The exhibition of closed-torus LD-RBC model which has a very good agreement with that which provided by Pan [34]

3. Results of parameters affecting the geometry of the RBC

Determination of the RBC radius is essential for modelling, especially when using LD model, where particle radius affects, for example, the values of the forces and momenta applied on each particle. In addition, knowing the RBC radius is a prerequisite for scaling and converting the DPD dimensions to physical units. So assessing this radius and identifying the factors affecting this parameter seems necessary. To measure the radius of modelled RBC, it is sufficient to calculate the longest distance between the centers of particles positioned on a RBC diameter. For example, the values of parameters listed in Table 1 are used for the RBC shown in Fig. 2.

Table 1.
Parameters of conservative force [(in (4)], WLC spring force and bending resistance used for RBC simulation

k_b	λ_p	L_{max}	a (4)	N_c
50	0.0005	1.3	500	10

The radius of modelled RBC was calculated using the parameters in Table 1. Fig. 3 shows the changes in the radius size with time in during the construction. The fluctuations observed in the early steps are related to moments when colloidal particles of RBC have not yet reached equilibrium, or in other words, the red blood cell has not yet formed. This is because in each simulation, the distribution of colloids constituting the red blood cell is initially random and reaches the equilibrium during the process.

After several RBC simulations, it was observed that factors such as the coarse graining parameter (N_c), conservative force coefficient [a in (4)] and parameters in WLC spring force like persistence length and maximum allowed length (L_{max}) affect the size of modeled red blood cell; as changing them led to variations in the RBC radius. Different simulations were conducted by different values of these parameters to observe the mechanism of their effect on the size of RBC radius. Note that since the purpose of the simulations was to investigate specific parameters, other factors were kept constant at values given in Table 1.

A) Impact of N_c on the size of modeled RBC

First, the influence of parameter N_c was investigated. For this purpose, simulations were conducted with values shown in Table 1 and different values of N_c. The simulations results are shown in Table 2, and plotted in Fig. 4.

The results of Table 2 and the corresponding plot clearly show the increase in RBC radius with the increase of N_c value. There is an obvious geometry-based justification for this increase in the RBC radius. As increasing the number of colloids in each red blood cell while keeping other parameters constant means that the distance between the centers of consecutive colloids (spring length) remains almost constant, and only the angle between the lines connecting the centers of adjacent colloids (angle θ) in the RBC decreases. This leads to an increase in the radius of modelled red blood cell (see Fig. 2).

B) Effect of conservative force coefficient on the size of modeled RBC

Another parameter whose effect on RBC radius needs to be considered is the conservative force coefficient [(a in (4)]. During the modelling, Equation 4 must be used for the conservative force for colloids of a single red blood cell. The colloids that are in different red blood cells must be modelled with the force expressed in form of (8). The RBC radius was calculated with different values for conservative force coefficient [(a in (4)] and the results are shown in Table 3, and plotted in Fig. 5. This figure shows a direct relationship between the conservative force coefficient and the RBC radius.

To determine the reasons behind the increasing trends observed in the Fig. 5, the equilibrium length between two adjacent colloids of an RBC was examined. In an RBC which is in equilibrium, two kinds of forces include of linear conservative forces (as the repulsive forces) and WLC spring forces (as the attractive forces) lead to a certain equilibrium distance between adjacent colloids.

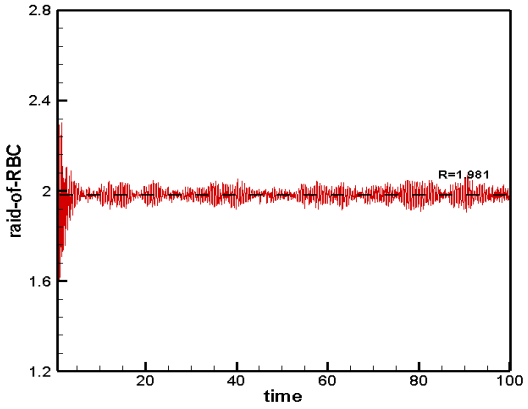

Fig. 3. Time evolution of the size of RBC radius based on the parameters listed in Table 1

Table 2
Effect of coarse graining parameter (N_c) on the radius of modeled RBC.

Coarse graining parameter (N_c)	*The radius of modeled RBC*
6	1.29
10	1.98
20	3.81

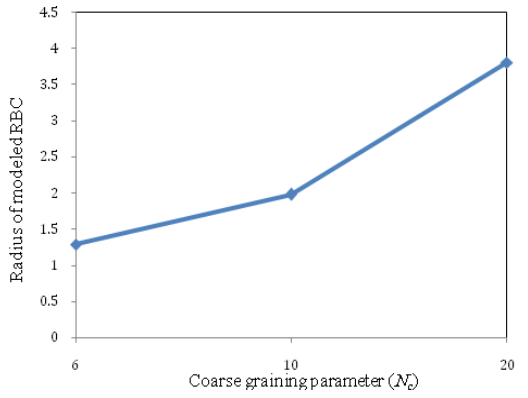

Fig. 4. Effect of parameter N_c on the radius of modelled RBC

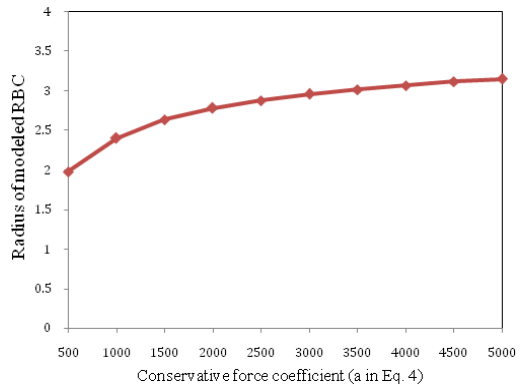

Fig. 5. Radius of modeled RBC as a function of conservative force coefficient (a in Equation 4).

Table 3
Effect of conservative force coefficient [a in (4)] on the radius of modeled RBC

The conservative force coefficient [a in (4)]	*The radius of modeled RBC*
500	1.98
1000	2.4
1500	2.64
2000	2.78
2500	2.88
3000	2.96
3500	3.02
4000	3.07
4500	3.12
5000	3.15

In Figs 6 and 7, the difference between these two forces are plotted against the distance between the centers of two neighbouring colloids with coefficients of a=500 and a=2000. Comparing these two plots shows that the equilibrium distance (in which the resultant of two forces is zero, or F^{WLC}-F^{C}=0) increases with the increase of conservative force coefficient. In fact, spring forces that act as attractive force between two adjacent colloids in an RBC are responsible for keeping the particles integrated. Here, for any given spring force, an increase in conservative force coefficient (which acts as a repulsive force against the spring force between the colloids) leads to an increase in equilibrium distance between two adjacent colloids in an RBC.

Fig. 8, shows the changes in equilibrium distance versus changes in conservative force coefficient [(a in (4)] shows the same behavior observed in Fig. 5 for RBC radius. Fig. 5 and Fig. 8 show that from a=500 to a=1000 equilibrium distance between adjacent colloids and RBC radius have undergone drastic but similar changes. Both figures also show a rather sharp increase in equilibrium distance and RBC radius until a=3500; the point beyond which both parameters have undergone a gradual decline.

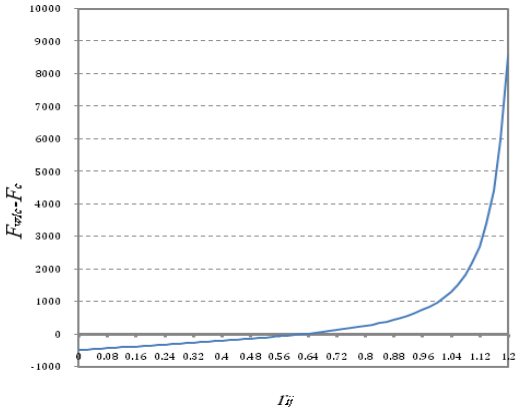

Fig. 6. Difference between linear conservative force and WLC spring force versus the distance between centers of two adjacent colloids with a=500 in (4)

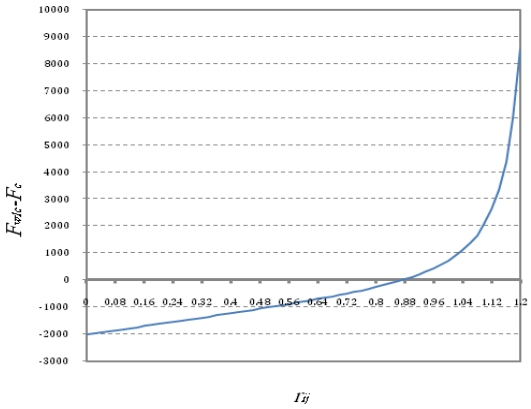

Fig. 7. Difference between linear conservative force and WLC spring force versus the distance between centers of two adjacent colloids with a=2000 in (4)

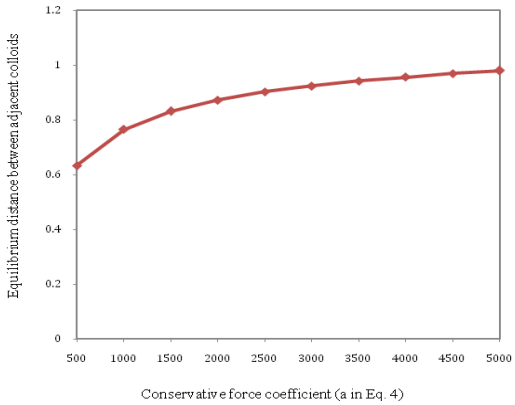

Fig. 8. Equilibrium distance between two adjacent colloids in an RBC versus changes in conservative force coefficient

C) The effects of spring force parameters on the size of modeled RBC

This section discusses the effect of the two parameters of WLC spring force, i.e. the persistence length and maximum allowed length (L_{max}) on the size of the modelled red blood cell. The results of performed simulations show that RBC size increases with the increase of both parameters. The trends of

increase in the RBC size due to increase in persistence length (λ_p) and maximum allowed length (L_{max}) are shown, respectively, in Figs 9 and 10. The increase in both coefficients of WLC spring force has resulted in weaker binding force, whereas the linear conservative force acting as the repulsive force between the two adjacent colloids has remained constant. As a result, the distance between the two adjacent colloids (spring length) in an RBC has increased, and this has led to an increase in its radius. The independent impact of each coefficient on the equilibrium length was also investigated, and the results were plotted in in Figs 11 and 12. These figures show that, as expected, the increase in each parameter leads to larger spring length between two adjacent colloids in a red blood cell.

4. Conclusion

In biological flows in main arteries which are required an explicit modelling of red blood cells, simulating of a single RBC in molecular levels, can be expressed with hundreds to tens of thousands of particles. Representation of this multi-particle simulation is so expensive. For example, simulating the flow in a 500µm long and 50µm in diameter arteriole in which only 35% of volume has been occupied by RBCs require simulating millions to hundreds of millions of particles. In the present work, we use a low-dimension (LD) model based on dissipative particle dynamics (DPD) which is introduced for the first time by Pan et al. This model is an effective approach to overcome the problem of high computational cost associated with the simulation of red blood cells and despite the methods like DPD which assume point particles, uses spherical particles include of specific radius. In this model, the number of particles required for simulation and thus the computational cost associated with modelling of larger vessels are decreased based on assumption of a radius for each particle. This RBC modelling in this work consists of only 10 colloidal particles that have been attached to each other by worm-like chain (WLC) springs. To model the bending rigidity of red blood cells, bending resistance is incorporated into the ring model as an angular bending force. In fact, a fundamental parameter in this model over existing mesoscale methods is the radius of the particles. The particle radius is considered as an input parameter and plays a decisive role, for example, in calculating the values of the forces and momenta applied to each particle. In addition, during scaling and converting the DPD dimensions into physical units, the radius of red blood cell needs to be known. After several RBC simulations, it was observed that factors such as the coarse graining parameter (N_c), affect the size of modelled red blood cell and led to increase the radius. As increasing the number of colloids in each red blood cell while keeping other parameters constant means that the distance between the centers of consecutive colloids (spring length) remains almost constant, and only the angle between the lines connecting the centers of adjacent colloids (angle θ) in the RBC decreases. This leads to an increase in the radius of modelled red blood cell (see Fig. 2). Another parameter we investigate the effect of that is the conservative force coefficient [(a in (4)]. Increasing this coefficient results in augmentation the radius of the RBCs. It was said this increase is because of the increment in the equilibrium distance between two adjacent colloids in an RBC. The last parameters peruse the effects were the coefficients in WLC spring force like persistence length and maximum allowed length (L_{max}). Increasing these two parameters led to weaken the spring force and therefore the increment in the equilibrium distance between two adjacent colloids in an RBC and increase in the radius of the RBCs.

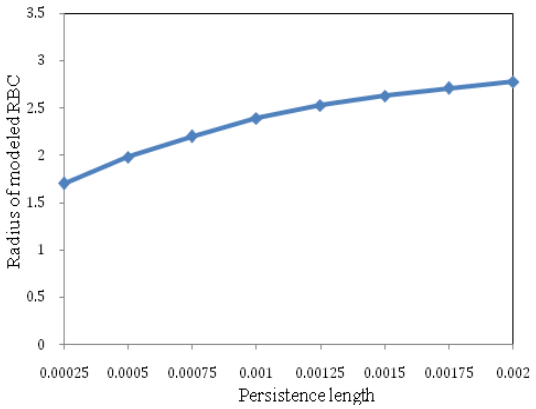

Fig. 9. Radius of modeled RBC as a function of persistence length (λ_p)

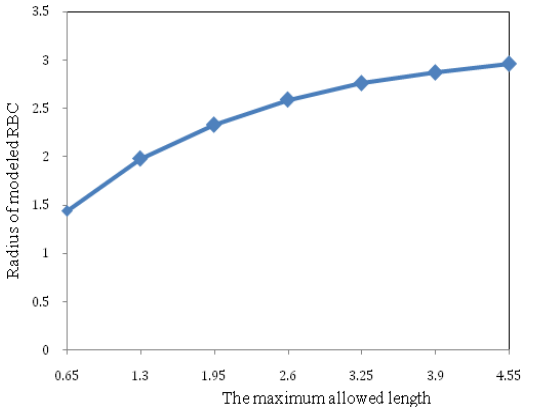

Fig.10. Radius of modeled RBC as a function of maximum allowed length (L_{max})

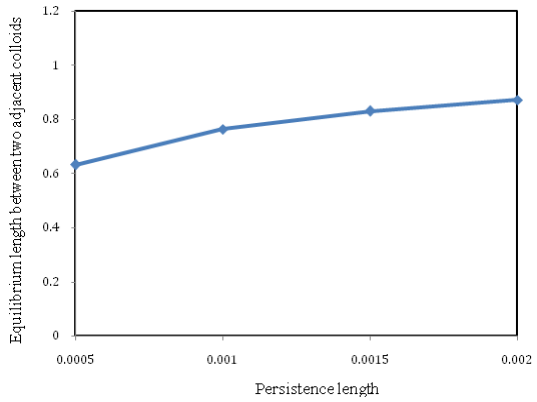

Fig. 11. Spring length (equilibrium length) between two adjacent colloids in a red blood cell as a function of persistence length (λ_p)

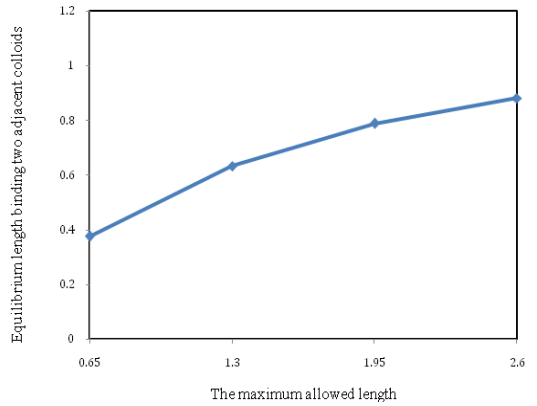

Fig. 12. Spring length (equilibrium length) binding two adjacent colloids in a red blood cell as a function of maximum allowed length (L_{max})

Appendix

r_c	cut-off radius
$\vec{v}_{ij}$	translational velocity of particle i relative to j
$g_{ij}^{\parallel}$, $g_{ij}^{\wedge}$	drag coefficients
$\vec{F}_{ij}^{U}$	conservative force
$\vec{F}_{ij}^{T}$	translational force
$\vec{F}_{ij}^{R}$	rotational force
$\vec{F}_{ij}^{\%}$	random force
$\vec{v}_i$	linear velocity
$\vec{\Omega}_i$	angular velocity
k_b	bending stiffness
q_{ijk}	angle between two consecutive springs or the inner product of $\vec{r}_{ij}$ and $\vec{r}_{jk}$

References

[1] T. Wang, S. Lü, Y. Hao, Z. Su, M. Long, Y. Cui, “Influence of microflow on hepatic sinusoid blood flow and red blood cell deformation”, Biophysical Journal, vol. 120, no. 21, pp. 4859-4873, Nov. 2021 (doi: 10.1016/j.bpj.2021.09.020).

[2] Y. Jo, H. Ahn, K. Shin, H. Lee, "Effects of pulsed magnetic field on the flowing red blood cells using microvascular model", IEEE Trans. on Magnetics, vol. 54, no. 11, pp. 1-3, Nov. 2018 (doi: 10.1109/TMAG.2018.2850927).

[3] G. Mchedlishvili, N. Maeda, “Blo o d flow structure related to red cell flow: A determinant of blood fluidity in narrow microvessels”, Japanese Journal of Physiology, vol. 51, no. 1, pp. 19–30, Feb. 2001 (doi: 10.2170/jjphysiol.51.19).

[4] C. Saldanha, “Hemorheology, microcirculation and macrocirculation”, Revista Portuguesa de Cardiologia, vol. 39, no. 1, pp. 25-26, Jan. 2020 (doi: 10.1016/j.repce.2020.04.002).

[5] A.S. Pop el and P. C. Johnson. “Microcirculation and hemorheology”, Annual Review of Fluid Mechanics, vol. 37, pp. 43–69, Jan. 2005 (doi: 10.1146%2Fannurev.fluid.37.042604.133933).

[6] M.R. Eid, K.L. Mahny, A.F. Al-Hossainy, “Homogeneous-heterogeneous catalysis on electromagnetic radiative Prandtl fluid flow: Darcy-Forchheimer substance scheme”, Surfaces and Interfaces, vol. 24, Article Number: 101119, June 2021 (doi: 10.1016/j.surfin.2021.101119)..

[7] S. Yaghoubi, E. Shirani, A. Pishevar, “Improvement of dissipative particle dynamics method by taking into account the particle size”, ***Scientia Iranica***, vol. 26, no. 3, pp. 1438-1445, May/June 2019 (doi: 10.24200/sci.2018.21042).

[8] W. Pan, D.A. Fedosov, G.E. Karniadakis, B. Caswell, “Hydrodynamic interactions for single dissipative-particle-dynamics particles and their clusters and filaments”, Physical Review, vol. 78, no. 4, Article Number: 046706, Oct. 2008 (doi: 0.1103/PhysRevE.78.046706).

[9] D.A. Fedosov, W. Pan, B. Caswell, G. Gompper, G.E. Karniadakis, “Predicting human blood viscosity in silico”, Proceedings of the National Academy of Sciences of the United States of America, vol. 108, no. 29, pp. 11772–11777, July 2011 (doi: 10.1073/pnas.1101210108).

[10] J.R. Clausen, D.A. Reasor, C.K. Aidun, “Parallel performance of a lattice-boltzmann/finite element cellular blood flow solver on the IBM blue gene/P architecture”, Computer Physics Communications, vol. 181, no. 6, pp. 1013-1020, June 2010 (doi: 10.1016/j.cpc.2010.02.005).

[11] J.P. Hale, G. Marcelli, K.H. Parker, C.P. Winlove, P.G. Petrov, “Red blood cell thermal fluctuations: comparison between experiment and molecular dynamicssimulations”, Soft Matter, vol. 5, no. 19, pp. 3603–3606, 2009 (doi: 10.1039/B910422D).

[12] J. Li, M. Dao, C.T. Lim, S. Suresh, “Spectrin-level modeling of the cytoskeletonand optical tweezers stretching of the erythrocyte”, Biophysical Journal, vol. 88, no. 5, pp. 3707–3719, May 2005 (doi: 10.1529/biophysj.104.047332).

[13] Y. Li, W. Li, L. Wan, Y. Xi, N. Wang, “Numerical simulation of boiling two-phase flow in the subchannel under static state and rolling motion”, International Journal of Heat and Mass Transfer, vol. 163, Article Number: 120416, Dec. 2020 (doi: 10.1016/j.ijheatmasstransfer.2020.120416).

[14] A. Karmakar, S. Acharya, “Numerical simulation of falling film flow hydrodynamics over round horizontal tubes”, International Journal of Heat and Mass Transfer, vol. 173, Article Number: 121175, July 2021 (doi: 10.1016/j.ijheatmasstransfer.2021.121175).

[15] L. Vaiani, E. Migliorini, E.A. Cavalcanti-Adam, A.E. Uva, M. Fiorentino, M. Gattullo, V.M. Manghisi, A. Boccaccio, “Coarse-grained elastic network modelling: A fast and

stable numerical tool to characterize mesenchymal stem cells subjected to AFM nanoindentation measurements", Materials Science and Engineering: C, vol. 121, Article Number: 111860, Feb. 2021 (doi: 10.1016/j.msec.2020.111860).

[16] M. Razizadeh, M. Nikfar, R. Paul, Y. Liu, "Coarse-grained modeling of pore dynamics on the red blood cell membrane under large deformations, Biophysical Journal, vol. 119, no. 3, pp. 471-482, Aug. 2020 (doi: 10.1016/j.bpj.2020.06.016).

[17] N. Hori, M.E. Rosti, S. Takagi, "An Eulerian-based immersed boundary method for particle suspensions with implicit lubrication model", Computers and Fluids, vol. 236, Article Number: 105278, March 2022 (doi: 10.1016/j.compfluid.2021.105278).

[18] W. Dzwinel, K. Boryczko, D.A. Yuen, "A discrete-particle model of blood dynamics in capillary vessels", Journal of Colloid and Interface Science, vol. 258, no. 1, pp. 163–173, Feb. 2003 (doi: 10.1016/S0021-9797(02)00075-9).

[19] S. Ma, S. Wang, X. Qi, K. Han, X. Jin, Z. Li, G. Hu, X. Li, "Multiscale computational framework for predicting viscoelasticity of red blood cells in aging and mechanical fatigue", Computer Methods in Applied Mechanics and Engineering, vol. 391, Article Number: 114535, March 2022 (doi: 10.1016/j.cma.2021.114535).

[20] C. Kotsalos, J. Latt, B. Chopard, "Bridging the computational gap between mesoscopic and continuum modeling of red blood cells for fully resolved blood flow", Journal of Computational Physics, vol. 398, Article Number: 108905, Dec. 2019 (doi: 10.1016/j.jcp.2019.108905).

[21] M. Dhahbi, M. Ben Chiekh, B. Gilles, J.C. Béra, A. Jemni, "Numerical simulations of particle dynamics in a poststenotic blood vessel region within the scope of extracorporeal ultrasound stenosis treatment", Medical Engineering and Physics, vol. 34, no. 7, pp. 982-989, Sept. 2012 (doi: 10.1016/j.medengphy.2011.11.003).

[22] D.A. Fedosov, B. Caswell, G.E. Karniadakis, "A multiscale red blood cell model with accurate mechanics, rheology, and dynamics", Biophysical Journal, vol. 98, no. 10, pp. 2215-2225, May 2010.

[23] J. Zhang, P.C. Johnson, A.S. Popel, "Effects of erythrocyte deformability and aggregation on the cell free layer and apparent viscosity of microscopic blood flows", Microvascular Research, vol. 77, no. 3, pp. 265–272, May 2009 (doi: 10.1016/j.mvr.2009.01.010).

[24] M. Alafzadeh, S. Yaghoubi, E. Shirani, M. Rahmani, "Simulation of RBC dynamics using combined low dimension, immersed boundary and lattice Boltzmann methods", Molecular simulation, 2019, (doi:10.1080/08927022.2019.1643018).

[25] I.V. Pivkin, G.E. Karniadakis, "Accurate coarse-grained modeling of red blood cells", Physical Review Letters, vol. 101, no. 11, :118105, 2008.

[26] A. Tarakanova, J. Ozsvar, A.S. Weiss, M.J. Buehler, "Coarse-grained model of tropoelastin self-assembly into nascent fibrils", Materials Today Bio, vol. 3, Article Number: 100016, June 2019 (doi: 10.1016/j.mtbio.201-9.100016).

[27] H. Fellermann, S. Rasmussen, H. Ziock, R.V. Solé, "Life cycle of a minimal protocell- A dissipative particle dynamics study", Artificial Life, vol. 13, no. 4, pp. 319-345, Oct. 2007 (doi: 10.1162/artl.2007.13.4.319).

[28] K.P. Santo, A.V. Neimark, "Dissipative particle dynamics simulations in colloid and Interface science: A review", Advances in Colloid and Interface Science, vol. 298, Article Number: 102545, Dec. 2021 (doi: 10.1016/j.cis.2021.102545)..

[29] W. Pan, I.V. Pivkin, G.E. Karniadakis, "Single-particle hydrodynamics in DPD: A new formulation", Europhysics Letters, vol. 84, no. 1, Article Number: 10012, 2008.

[30] V. Pryamitsyn, V. Ganesan, "A coarse-grained explicit solvent simulation of rheology of colloidal suspensions", Journal of Chemical Physics, vol. 122, no. 10, Article Number: 104906, 2005 (doi: 10.1063/1.1860557).

[31] X. Fan, N. Phan-Thien, S. Chen, X. Wu, T.Y. Ng, "Simulating flow of DNA suspension using dissipative particle dynamics", Physics of Fluids, vol. 18, no. 6, Article Number: 063102, 2006 (doi: 10.1063/1.2206595).

[32] S. Yaghoubi, E. Shirani, A.R. Pishevar, Y. Afshar, "New modified weight function for the dissipative force in the DPD method to increase the Schmidt number", Europhysics Letters, vol. 110, no. 2, Article Number: 24002, 2015.

[33] W. Pan, B. Caswell, G.E. Karniadakis, "Rheology, microstructure and migrationin brownian colloidal suspensions", Langmuir, vol. 26, no. 1, pp. 133–142, Jan. 2010 (doi: 10.1021/la902205x).

[34] W. Pan, "Single particle DPD: Algorithms and applications", Ph.D. Thesis, University of Brown, Brown, May 2010. [1] W. Pan, B. Caswell, G.E. Karniadakis, "A low-dimensional model for the red blood cell", Soft Matter, vol. 6, no. 18, Article Number: 24282440, June 2010 (doi: 10.1039/C0SM00183J).